

# Globally Convergent Method for Optimal Control of Hybrid Dynamical Systems

Saif R. Kazi\* Mandar Thombre\*\* Lorenz Biegler\*\*\*

\* T-5 Applied Mathematics and Plasma Physics, Los Alamos National Laboratory, Los Alamos, NM 87545, USA (e-mail: skazi@lanl.gov)

\*\* Technological, Digital and Innovation, Equinor, Oslo, Norway (e-mail: mnth@equinor.com)

\*\*\* Department of Chemical Engineering, Carnegie Mellon University, Pittsburgh, PA 15213, USA (e-mail: lb01@andrew.cmu.edu)

**Abstract:** Optimal control of a Hybrid Dynamical System is a difficult problem because of unknown non-differentiable points or switches in the solution of discontinuous ODEs. The optimal control problem for such hybrid dynamical system can be reformulated into a dynamic complementarity system (DCS) problem. In this paper, a moving finite element with switch detection method is implemented to ensure higher order accuracy for numerical discretization schemes such as Implicit Runge Kutta (IRK) or Orthogonal Collocation method. The DCS problem is solved using a globally convergent nonlinear complementarity solver based on active set strategy to avoid spurious stationary solutions.

*Keywords:* Differential Complementarity System, Hybrid Dynamical Systems, Complementarity Constraints

## 1. INTRODUCTION

Hybrid Dynamical Systems are systems where the state dynamics are both continuous and discrete depending on the value of the state solution. They are commonly found in robotics engineering applications (Patel et al. (2019); Raghunathan et al. (2022)) and chemical process control problems (Baumrucker and Biegler (2009); Raghunathan et al. (2004); Moudgalya and Jaguste (2001)).

A typical Hybrid Dynamical System can be represented as ODEs with discontinuous right-hand side as:

$$\dot{x} = f_i(x(t), u(t)), \text{ if } x(t) \in R_i \subset \mathbb{R}^{n_x}, \quad i \in \mathcal{F} = \{1, \dots, n_f\} \quad (1)$$

where  $R_i$  denote the regions (disjoint sets) in the state space and  $f_i(\cdot)$  are corresponding smooth functions representing the state dynamics in them.  $n_f$  is the number of piecewise functions and  $u(t)$  denotes the external control input in the system.

Hybrid Dynamical Systems were extensively studied by Filippov (1960), who proposed a formulation using the convex combination to transform (1) as

$$\dot{x} = \sum_{i \in \mathcal{F}} \nu_i f_i(x, u), \quad \sum_{i \in \mathcal{F}} \nu_i = 1, \nu_i \geq 0, \nu_i = 0 \text{ if } x(t) \notin R_i \quad (2)$$

$\nu_i$  are also called *convexification variables* or *Filippov multipliers*. The convexification allows to write the piecewise formulation (1) with disjoint sets into a continuous algebraic form (2) where the system dynamics at the boundary region  $\{x \in R_i \cap R_j\}$  is well defined, i.e.  $\dot{x} = \nu_i f_i + \nu_j f_j$ ,

\* Work at Los Alamos National Laboratory is done under the auspices of the National Nuclear Security Administration under U.S. D.O.E. Contract No. 89233218CNA000001.

$\nu_i + \nu_j = 1$ , which is more suitable for continuous optimization solvers. Stewart (1990) presented an extension with *indicator functions* ( $g_i(x)$ ) for the disjoint sets ( $R_i$ ):

$$R_i = \{x \in \mathbb{R}^{n_x} | g_i(x) < \min_{j \in \mathcal{F}, j \neq i} g_j(x)\} \quad (3)$$

Under mild assumptions such as  $g(\cdot)$  and  $\nabla g(\cdot)$  are Lipschitz continuous and sufficiently smooth, the Filippov system can be reformulated as:

$$\dot{x} = \sum_{i \in \mathcal{F}} \nu_i f_i(x, u) \quad (4a)$$

where the *Filippov multipliers* are algebraic variables determined by the following parametric linear program (LP)

$$\text{LP}(x) : \nu(x) = \arg \min_{\nu} g(x)^T \nu \text{ s.t. } \sum_{i \in \mathcal{F}} \nu_i = 1, \nu_i \geq 0 \quad (4b)$$

Here, the parametric LP solution ( $\nu(x)$ ) is dependent on the state variable ( $x$ ), which itself is a primal variable in the optimal control problem. The linear program (4b) needs to be reformulated using its KKT conditions for the optimal control problem to be represented as a single-level optimization problem. Thus, the hybrid dynamic constraints in the problem can be rewritten into a dynamic complementarity system (DCS) as follows:

$$\dot{x} = \sum_{i \in \mathcal{F}} \nu_i f_i(x, u), \quad (5a)$$

$$g(x) - \lambda - \mu e = 0, \quad (5b)$$

$$\sum_{i \in \mathcal{F}} \nu_i = 1, \quad 0 \leq \nu \perp \lambda \geq 0 \quad (5c)$$

where  $g(x) = [g_1(x), \dots, g_{n_f}(x)]^T$ ,  $e = [1, \dots, 1]^T$  denote the indicator functions and the unit vector, whereas  $\nu, \lambda \in$

$\mathbb{R}^{n_f}, \mu \in \mathbb{R}$  denote the complementing variables and Lagrange multipliers, respectively.

The complementarity operator ( $\perp$ ) for two vectors  $\nu$  and  $\lambda$  denotes the following relation:

$$0 \leq \nu \perp \lambda \geq 0 \iff \nu, \lambda \geq 0, \nu^T \lambda = 0 \quad (6)$$

Since both vectors are non-negative, the relation is equivalent to  $\nu_i \lambda_i = 0$  or  $\min(\lambda_i, \nu_i) = 0 \quad \forall i \in \mathcal{F}$

## 2. OPTIMAL CONTROL OF DYNAMIC COMPLEMENTARITY PROBLEM

The optimal control problem for hybrid dynamic systems is described as an infinite dimensional optimization problem with complementarity constraints as shown here:

$$\min_u \Phi(x(t_f)) + \int_0^{t_f} \Psi(x, u) dt \quad (7a)$$

$$\text{s.t. } \dot{x} = \sum_{i \in \mathcal{F}} \nu_i f_i(x, u), \quad x(0) = x_0 \quad (7b)$$

$$g(x) - \lambda - \mu e = 0, \quad (7c)$$

$$\sum_{i \in \mathcal{F}} \nu_i = 1, 0 \leq \nu \perp \lambda \geq 0, \quad t \in [0, t_f] \quad (7d)$$

The objective function can consist of both terminal cost function ( $\Phi$ ) and state cost function ( $\Psi$ ) depending on the type of application. The above formulation can also be thought of as a differential-algebraic equation (DAE) based optimization problem where the complementarity constraints are reformulated into algebraic inequalities (or equalities). There are two ways to solve DAE optimization problem: 1) *optimize - then - discretize* and 2) *discretize - then - optimize*, where the former solves the first order Euler-Lagrange conditions, which results in a system of coupled forward backward adjoint boundary value problem (BVP). This method is difficult to implement for general optimal control problems and doesn't provide an optimality guarantee for the solution. On the other hand, *discretize - then - optimize* is a more flexible approach where the DAE based constraints are discretized to nonlinear algebraic constraints and solved as a large scale nonlinear program (NLP) using standard NLP solvers.

### 2.1 Discretization

Numerical discretization schemes such as Implicit Runge Kutta (IRK) methods or Orthogonal Collocation on Finite Elements (OCFE) can be used to discretize differential equations with high accuracy solutions. These methods use Taylor series approximation of the solution and internal stages or collocation points inside each time finite element  $[t_i, t_{i+1}]$  to reformulate the differential equations into discretized equations.

For brevity we define  $F = [f_1, \dots, f_{n_f}]$  and rewrite (7b) & (7d) as  $\dot{x} = F(x, u)\nu$ , and  $e^T \nu = 1$

For  $i = 0, \dots, N - 1, \quad k = 1, \dots, K$

$$x_{i+1,0} = x_{i,0} + h \sum_{k=1}^K b_k F_{i,k} \nu_{i,k}, \quad (8a)$$

$$x_{i,k} = x_{i,0} + h \sum_{k=1}^K a_{i,k} F_{i,k} \nu_{i,k}, \quad (8b)$$

$$g(x_{i,k}) - \lambda_{i,k} - \mu_{i,k} e = 0, \quad (8c)$$

$$e^T \nu_{i,k} = 1, \quad x_{0,0} = x_0, \quad (8d)$$

$$0 \leq \nu_{i,k} \perp \lambda_{i,k} \geq 0 \quad (8e)$$

where  $N$  is number of finite elements and  $K$  is the number of internal collocation points or stages.  $a_{i,k}$  and  $b_k$  are constant parameters depending on the discretization scheme.  $h$  refers to the uniform step size equal to  $\frac{t_f}{N}$  in this case.

### 2.2 Non-uniform Step Size

For standard IRK discretization scheme, the step size  $h$  typically is chosen constant. The standard assumption in numerical methods such as IRK or OCFE is the smoothness of the solution inside the time interval finite elements. But, the solution of the hybrid dynamic system is known to be non-smooth at unknown time points i.e. switch points. To ensure that the solution  $x_{i,k}$  is only non-smooth at the boundary of the finite element and satisfy smoothness property required for discretization schemes, Baumrucker and Biegler (2009) proposed using a non-uniform step size  $h_i$  as a free variable in the optimization problem. Moreover, they also reformulated the complementarity constraint using cross-complementarity constraints such that the active-set of the constraint only changes at the finite element boundary.

For  $i = 0, \dots, N - 1, \quad k = 1, \dots, K$

$$x_{i+1,0} = x_{i,0} + h_i \sum_{k=1}^K b_k F_{i,k} \nu_{i,k}, \quad (9a)$$

$$x_{i,k} = x_{i,0} + h_i \sum_{k=1}^K a_{i,k} F_{i,k} \nu_{i,k}, \quad (9b)$$

$$\sum_{i=0}^{N-1} h_i = t_f, \underline{h} \leq h_i \leq \bar{h}, \quad (9c)$$

$$g(x_{i,k}) - \lambda_{i,k} - \mu_{i,k} e = 0, \quad (9d)$$

$$e^T \nu_{i,k} = 1, \quad x_{0,0} = x_0, \quad (9e)$$

$$0 \leq \nu_{i,k} \perp \sum_{k=1}^K \lambda_{i,k} \geq 0 \quad (9f)$$

The bounds on the step size ensured that the element boundaries don't coincide with each other and the problem is well-conditioned.

### 2.3 Step Equilibration

Although, the above reformulation ensures that the switching points in the solution coincide with the element boundaries, the number of degrees of freedom is more than in the original problem. This is because of the additional variables  $h_i$  and only one additional equality constraint (9c) in the formulation. To ensure that the number of degrees of freedom is consistent and the state

solution is unique, Nurkanović et al. (2022) proposed a step-equilibration approach where they added  $N - 1$  constraints using an indicator function ( $\eta$ ) which is only non-zero when there is an active-set change in complementarity constraint.

We define the following auxiliary variables  $\hat{\lambda}_i$  and  $\hat{\nu}_i$  as:

$$\hat{\lambda}_i = \sum_{k=1}^K \lambda_{i,k}, \quad \hat{\nu}_i = \sum_{k=1}^K \nu_{i,k} \quad (10a)$$

Then, we use the Hadamard product of the forward and backward sum of the complementarity variables to determine if it has switched from positive to zero (or vice-versa).

$$\pi_i^\lambda = \hat{\lambda}_{i-1} \odot \hat{\lambda}_i, \quad \pi_i^\nu = \hat{\nu}_{i-1} \odot \hat{\nu}_i \quad (10b)$$

where  $\odot$  represents pointwise or element-wise product of vectors. Here, at least  $\pi_i^\lambda$  or  $\pi_i^\nu$  is zero at each element, and both are exactly zero at the element corresponding to the switching point. The sum of the two vectors is a good candidate for the indicator function

$$\tau_i = \pi_i^\lambda + \pi_i^\nu, \quad \eta_i = \prod_{j=1}^{n_\tau} \tau_i^{(j)} \quad (10c)$$

Since the indicator variable  $\eta_i$  is non-negative and only zero at the switching element, the relation between step size and indicator variable can be represented by the following complementarity constraints.

$$0 \leq (h_i - h_{i+1})^2 \perp \eta_i \geq 0, \quad i = 0, \dots, N - 2 \quad (10d)$$

The finite element with switch detection (FESD) algorithm was implemented as a package NOSNOC in Nurkanović and Diehl (2022).

### 3. GLOBAL CONVERGENT ALGORITHM

The large NLP with complementarity constraints is called a mathematical program with equilibrium constraints (MPEC), which is a non-smooth optimization problem given by:

$$\min_u \Phi(x_N) + \sum_{i=0}^{N-1} \sum_{k=1}^K w_{i,k} \Psi(x_{i,k}, u_{i,k}) \quad (11a)$$

$$\text{s.t. Eq.(9) - Discretized Equations,} \quad (11b)$$

$$\text{Eq.(10) - Step Equilibration} \quad (11c)$$

where  $w_{i,k}$  are the quadrature weight parameters that approximate the integration of the state cost function.

For simplicity, we rewrite the large scale MPEC (11) in a more general form:

$$\min_x f_{obj}(x) \quad (12a)$$

$$\text{s.t. } g_I(x) \leq 0, g_E(x) = 0, \quad (12b)$$

$$0 \leq G(x) \perp H(x) \geq 0 \quad (12c)$$

where the complementarity constraints (12d) represent the cross-complementarity constraints (9f) and step equilibration constraints (10d).

#### 3.1 Relaxation Approach

Since the MPEC (12) is inherently non-smooth, it is not possible to solve them in their original form using standard NLP solvers. Furthermore, any feasible point of

MPEC does not satisfy the basic constraint qualifications (LICQ and MFCQ) for KKT based solvers. Therefore, most methods reformulate and relax the complementarity constraint into an inequality (Reg( $\epsilon$ ), Scheel and Scholtes (2000)) or equality (RegEq( $\epsilon$ )) based constraints as:

$$G(x), H(x) \geq 0, \quad G(x)^T H(x) \leq \epsilon \text{ or } G_i(x)H_i(x) = \epsilon \quad (13)$$

Here  $\epsilon > 0$  is a positive relaxation parameter which allows the MPEC to be solved using NLP solvers. Typically MPECs are solved by sequentially solving the  $\epsilon$  relaxed NLP problem with decreasing values of  $\epsilon$ , by using the solution of the previous run as the initial guess for the NLP solver. Ralph and Wright (2004); Hoheisel et al. (2013) showed that the solutions of the relaxed NLPs in the neighborhood of the solution converges to a strong stationary point under certain conditions. Although these methods have local convergence properties near the solution point, they are not globally convergent and convergence to the *correct* solution depends on the starting guess to the NLP solver. As an example, consider the problem from Leyffer and Munson (2007):

$$\min (x - 1)^2 + (y - 1)^2 \text{ s.t. } 0 \leq x \perp y \geq 0 \quad (14a)$$

If the above MPEC is solved using Reg( $\epsilon$ ) by relaxing the complementarity constraint (14b) by the following inequality:

$$x, y \geq 0, \quad x^T y \leq \epsilon \quad (15)$$

then the KKT solution for the regularized problem is  $(\sqrt{\epsilon}, \sqrt{\epsilon})$  which will converge to the spurious solution at origin as  $\epsilon \rightarrow 0$  (see Fig.1). The relaxation only converges to the right solution (1, 0) or (0, 1) if the initial guess is close to the solution.

#### 3.2 Penalty Formulation

Other methods to solve MPEC include the penalty based formulation where the complementarity constraint is added as a penalty term multiplied by a parameter ( $\rho$ ) in the objective function.

$$\min_x f_{obj}(x) + \rho(G(x)^T H(x)) \quad (16a)$$

$$\text{s.t. } g_I(x) \leq 0, g_E(x) = 0, \quad (16b)$$

$$G(x) \geq 0, H(x) \geq 0 \quad (16c)$$

Hu and Ralph (2004) showed the convergence of the penalty methods if the penalty parameter was more than a critical value ( $\rho \geq \rho_c$ ) which depends on the value of the MPCC multipliers. Leyffer et al. (2006) proposed an update rule for the penalty parameter for global convergence of interior point methods for MPECs. Both results are based on strong assumptions of MPEC-LICQ and asymptotic weak non-degeneracy which are violated in most cases. Furthermore, the penalty formulation NLP (16) becomes ill-conditioned as the value of  $\rho$  increases.

#### 3.3 Hybrid Active-Set Strategy

Another method for global convergence of MPECs, proposed by Leyffer and Munson (2007), sequentially solves a linearized MPEC (LPEC) around a feasible point ( $x_k$ ) with an additional trust-region constraint.

$$\min_d \nabla f_{obj}(x_k)^T d \quad (17a)$$

$$\text{s.t. } \nabla g_I(x_k)^T d \leq 0, \nabla g_E(x_k)^T d = 0, \quad (17b)$$

$$0 \leq G(x_k) + \nabla G(x_k)^T d \perp H(x_k) + \nabla H(x_k)^T d \geq 0, \quad (17c)$$

$$\|d\| \leq \Delta_k \quad (17d)$$

where  $d$  represents the descent direction vector. Only the local optimal solution  $x^*$  satisfies the  $d = 0$  condition of zero descent direction. The algorithm updates the iterate  $x^k$  in the descent direction vector until it reaches some tolerance value ( $\|d\| \leq \epsilon_{tol}$ ). They also used a filter based on the complementarity violation to update the trust region radius ( $\Delta_k$ ), and showed that their method is globally convergent to the correct local optimal solution as the trust region radius decreases to zero asymptotically ( $\Delta_k \rightarrow 0$ ) under milder assumptions such as MPEC-MFCQ.

Although the method is globally convergent with nice theoretical properties, it still requires to solve a LPEC which is an NP-hard problem. The LPEC can also be formulated into a mixed integer linear program (MILP) using big-M formulation to transform the complementarity constraints.

$$0 \leq \nabla G(x_k)^T d \leq My, \quad y \in \{0, 1\}^{|G|} \quad (18a)$$

$$0 \leq \nabla H(x_k)^T d \leq M(e - y), \quad (18b)$$

where  $e = [1, \dots, 1]^T$ ,  $M > 0$  is the big-M parameter and  $y$  are the integer variables used to reformulate the complementarity constraint.

A significant drawback of this formulation is that the number of integer variables is equal to the number of complementarity constraints ( $|G| = |H| = q$ ). In the worst case scenario, this results in solving  $2^q$  linear programs (LPs) which is undesirable for large scale MPECs associated with hybrid dynamical systems. To overcome this drawback, we propose a hybrid active-set strategy which combines the faster convergence rate of the relaxation schemes and the robustness of the LPEC algorithm.

First, we solve the regularized problem  $\text{Reg}(\epsilon)$  with an initial point  $x_0$  and positive relaxation parameter  $\epsilon$ . Then, we identify the disjoint active-sets of the complementarity constraints at the solution ( $\hat{x}$ ). Unlike the penalty formulation, the error bounds between the regularized solution and the local optimal solution are bounded ( $\|\hat{x} - x^*\| = O(\epsilon^p)$ ) which makes the calculation of active sets using regularized solution more accurate.

$$I_\alpha = \{i, G_i(\hat{x}) = O(\epsilon), H_i(\hat{x}) > O(\epsilon)\}, \quad (19a)$$

$$I_\beta = \{i, G_i(\hat{x}) > O(\epsilon), H_i(\hat{x}) = O(\epsilon)\}, \quad (19b)$$

$$I_\gamma = \{i, G_i(\hat{x}) = O(\epsilon), H_i(\hat{x}) = O(\epsilon)\} \quad (19c)$$

Second, we formulate the MILP formulation of the MPEC at the solution ( $\hat{x}$ ). Instead of defining integer variables of each complementarity formulation, we reduce the set of integer variables by only defining them for the bi-active set ( $I_\gamma$ ). The reduced form of the MILP representation is given as:

$$\nabla G_i(x_k)^T d = 0 \quad i \in I_\alpha, \quad \nabla H_i(x_k)^T d = 0 \quad i \in I_\beta \quad (20a)$$

$$0 \leq \nabla G_i(x_k)^T d \leq My_i, \quad i \in I_\gamma \quad (20b)$$

$$0 \leq \nabla H_i(x_k)^T d \leq M(1 - y_i), \quad y_i \in \{0, 1\}, \quad i \in I_\gamma \quad (20c)$$

This reduces the number of integer variables from  $|G|$  to  $I_\gamma$ . In most cases, the bi-active set size is much smaller than the original number of complementarity constraints. Thus, the reduced MILP reformulation is easier to solve while conserving the robustness of the global convergence property.

We also note that if the bi-active set is empty, then the MILP reduces to a single LP to check for optimality condition at the solution ( $\hat{x}$ ). The full hybrid active-set strategy algorithm is presented here.

---

#### Algorithm 1 Hybrid Active-Set Strategy

---

```

Given  $x_0, \epsilon$  and  $\epsilon_{tol}$ 
while  $\epsilon \geq \epsilon_{tol}$  do
  Solve  $\text{Reg}(\epsilon_k)$  with  $x_k$  as the initial guess
  Calculate the active-set at the solution ( $\hat{x}$ ) using (19)
  if  $I_\gamma \neq \emptyset$  then
    Solve the MILP (17) with the reduced form (20)
     $x_{k+1} = x_k + \alpha_k d$ 
  else
     $x_{k+1} = \hat{x}$ 
  end if
   $\epsilon_k = \epsilon_k / Q$ 
   $k = k + 1$ 
end while

```

---

Here  $\alpha_k \in (0, 1]$  is a step-length parameter, determined by a line search.  $Q > 1$  is the decreasing ratio parameter for  $\epsilon$ , used as a constant hyperparameter.

We revisit the toy example from previous subsection to present the efficacy of the proposed strategy.

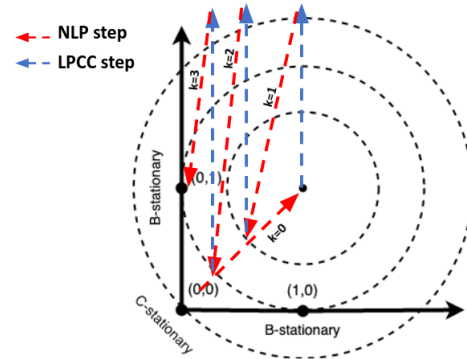


Fig. 1. Iteration trajectory with Algorithm 1

As can be seen in Fig.1, the proposed strategy converges to the correct solution of (1, 0) even when the initial guess is at origin. We observe that although the NLP step ( $\text{Reg}(\epsilon)$ ) outputs the  $(\sqrt{\epsilon}, \sqrt{\epsilon})$  initially, the MILP step pushes it away from the spurious solution and after three iterations, the point is close enough for the NLP relaxation problem to reach the optimal point at (1, 0).

Hybrid active-set strategies have been proposed earlier by Fukushima and Tseng (2002); Lin and Fukushima (2006) but they didn't use a LPEC or MILP formulation to verify optimality of the solution. Rather, they verify the non-negativity of the MPEC multipliers for each complementarity constraint, which can be computationally expensive for large MPEC problems.

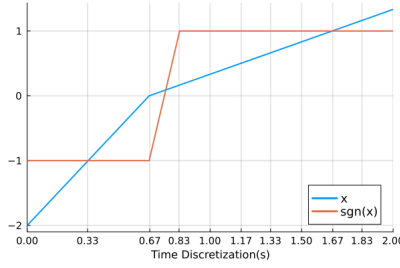


Fig. 2. Results for Signum Problem

#### 4. RESULTS

In this section, we implement the hybrid active-set strategy to dynamic complementarity problems derived from hybrid dynamic control problems. We used Julia 1.7 to model the problems using the Symbolics package library and used JuMP as the optimization modeling language. The regularized problems are solved in the nonlinear interior point solver IPOPT (Wächter and Biegler, 2006) and the HiGHS solver (Huangfu and Hall, 2018) is used to solve the MILP formulation.

##### 4.1 Signum Problem

The signum problem is a commonly used example for hybrid dynamic systems.

$$\min_x \phi(x(t_f)), \text{ s.t. } \dot{x} = 2 - \text{sgn}(x), x(0) = -2, t \in [0, 2] \quad (21a)$$

Although the problem has zero degrees of freedom, the problem is formulated as an optimization problem for illustrative purposes. The  $\text{sgn}(x)$  is a piecewise function described as:

$$\text{sgn}(x) = \begin{cases} -1 & x < 0, \\ [-1, 1] & x = 0, \\ 1 & x > 0 \end{cases} \quad (21b)$$

The piecewise formulation is reformulated as a DCS (5) using the complementarity constraints as:

$$\dot{x} = 3\nu_1 + \nu_2, \quad (21c)$$

$$x - \lambda_1 - \mu = 0, \quad (21d)$$

$$-x - \lambda_2 - \mu = 0, \quad (21e)$$

$$\nu_1 + \nu_2 = 1, 0 \leq \nu_i \perp \lambda_i \geq 0, i = 1, 2 \quad (21f)$$

We can substitute  $\nu_2 = 1 - \nu_1$  and subtract (21f) from (21f) to reduce the system as:

$$\dot{x} = 1 + 2\nu_1, \quad (21g)$$

$$2x - \lambda_1 + \lambda_2 = 0, \quad (21h)$$

$$0 \leq \nu_1 \perp \lambda_1 \geq 0, 0 \leq 1 - \nu_1 \perp \lambda_2 \geq 0 \quad (21i)$$

The dynamic constraints are discretized using the 4th order IRK discretization with  $N = 10$  finite elements. The plot in Fig.2 shows the profile of the state solution ( $x$ ) and the switching variable ( $\nu_1$ ). As can be seen in the figure, the switching time  $t_s = 2/3$  is correctly determined by the solver and ensures that the switch occurs at the element boundary.

##### 4.2 Ideal Gas-Liquid Closed System

Finally, we consider the ideal-gas liquid tank system from Moudgalya and Ryali (2001). In this example, there is

a closed tank with one feed inlet and one outlet with a control valve that regulates the pressure inside the vessel as shown in Fig.3.

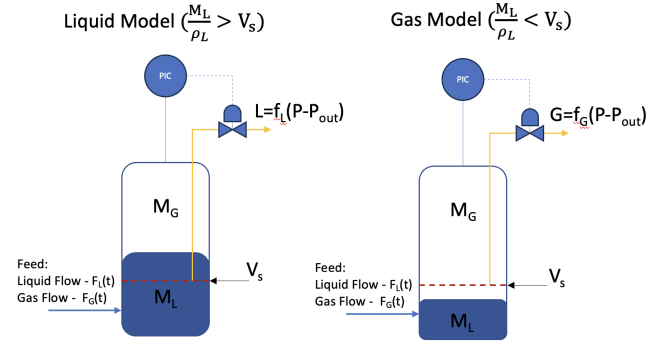


Fig. 3. An ideal gas-liquid system

The feed is a mixture of liquid ( $F_L$ ) and ideal gas ( $F_G$ ) and the outlet is either liquid ( $L$ ) or gas ( $G$ ) depending on whether the liquid level is above or below the outlet tube opening ( $V_s$ ). The modeling assumptions are:

- The gas and the liquid do not react
- The liquid has negligible vapor pressure
- The valve dynamics are ignored
- The flow rate through the valve is proportional to the difference of tank and outlet pressure
- The temperature, feed flow rates, outlet pressure and the valve opening are kept constant.

The dynamics of the system are described by the following set of differential equations.

$$\begin{aligned} \text{Liquid model: } (\frac{M_L}{\rho_L} > V_s) \quad & \text{Gas model: } (\frac{M_L}{\rho_L} < V_s) \\ \frac{dM_G}{dt} = F_G, \quad & \frac{dM_G}{dt} = F_G - G, \quad (22a) \\ \frac{dM_L}{dt} = F_L - L, \quad & \frac{dM_L}{dt} = F_L, \quad (22b) \\ M_G \frac{RT}{P} + \frac{M_L}{\rho_L} = V, \quad & (22c) \\ L = f_L(P - P_{out}) \quad & G = f_G(P - P_{out}) \quad (22d) \end{aligned}$$

The rate of liquid ( $M_L$ ) and vapor holdup ( $M_G$ ) vary according to the conservation-based differential equations (22a) and (22b). The total volume ( $V$ ) and the tank pressure ( $P$ ) are related to the ideal gas equation and liquid volume (22c). The liquid and vapor outlet flows are related as a function of ( $P - P_{out}$ ). The system parameter values in this example are listed in Table 1.

We reformulate the above dynamic system into a DCS using complementarity constraints as:

$$\frac{dM_G}{dt} = F_G\nu + (F_G - G)(1 - \nu), \quad (23a)$$

$$\frac{dM_L}{dt} = (F_L - L)\nu + F_L(1 - \nu), \quad (23b)$$

$$\frac{M_L}{\rho_L} - V_s = s_1 - s_2, \quad (23c)$$

$$0 \leq 1 - \nu \perp s_1 \geq 0, 0 \leq \nu \perp s_2 \geq 0, \quad (23d)$$

Here  $s_1$  and  $s_2$  are positive slack variables which denote the positive and negative part of the switching variable ( $\frac{M_L}{\rho_L} - V_s$ ) respectively.

Parameters	Value
$F_L, F_G$ (mol/sec)	2.5, 0.1
$V, V_s$ (litres)	10, 5
$T$ (K)	300
$P_{out}$ (atm)	1
$\rho_L$ (mol/l)	50
$f_L, f_G$	0.1

Table 1. Parameter values in Ideal Gas-Liquid Closed System

The initial conditions for the state variables are specified as:  $P_0 = 35\text{atm}$ ,  $M_{L_0} = 260\text{mol}$ ,  $M_{G_0} = 6.83\text{mol}$ ,  $L_0 = G_0 = 0.25\text{mol}$ . Similar to the first example, the dynamic constraints are discretized with  $N = 100$  finite elements and 4th order IRK discretization scheme for a time horizon  $t_f = 20\text{s}$ . The results from the optimization are plotted in the following figures in Fig.4 and 5. The switching time or point in this case ( $t_s = 9.37\text{s}$ ) can be clearly seen in both the plots. Initially, the system only has liquid exit as the liquid holdup is higher than the set point ( $V_s$ ), the switch happens when the liquid holdup ( $M_L = 250$ ,  $M_L/\rho_L = 5.0$ ) goes below the set volume ( $V_s$ ) and gas starts coming out from the outlet reducing the tank pressure as shown in Figure 5. The plots clearly show that our method is able to identify the switching point in the hybrid dynamics and adapt the time step sizes ( $h_i$ ) such that the switch time  $t_s$  occurs at the boundary of an element.

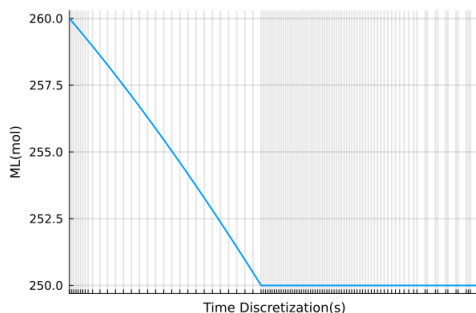


Fig. 4. Liquid holdup in the tank

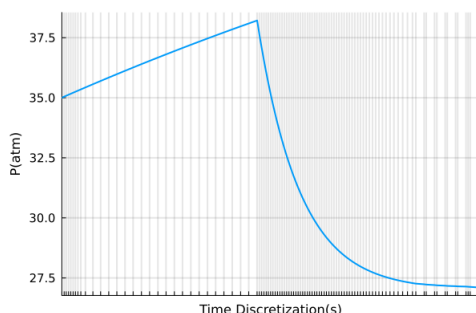


Fig. 5. Pressure profile inside the tank

## 5. CONCLUSION

This study presents a framework to solve hybrid dynamics as a dynamic complementarity system (DCS) problem.

Here complementarity constraints are used to determine moving finite elements with switch detection based constraints. The large scale complementarity constraint problem is solved using the hybrid active-set strategy to ensure global convergence to the local optimal solution. Two examples demonstrate that the proposed method is able to locate accurately the non-smoothness of the solution. In future work, we will use our algorithm to solve different types of hybrid dynamics problem, including state jump discontinuities and sliding mode control for multiple types of application problems.

## ACKNOWLEDGEMENTS

The work by Saif R. Kazi was supported by the US Department of Energy through the Center of Nonlinear Studies (CNLS) in Los Alamos National Laboratory.

## REFERENCES

- Baumrucker, B. and Biegler, L.T. (2009) *Journal of Process Control*, 19(8), 1248–1256.
- Filippov, A.F. (1960) *Matemat. sbornik*, 93(1), 99–128.
- Fukushima, M. and Tseng, P. (2002) *SIAM Journal on Optimization*, 12(3), 724–739.
- Hoheisel, T., Kanzow, C., and Schwartz, A. (2013) *Mathematical Programming*, 137, 257–288.
- Hu, X.M. and Ralph, D. (2004) *Journal of Optimization Theory and Applications*, 123, 365–390.
- Huangfu, Q. and Hall, J.J. (2018) *Mathematical Programming Computation*, 10(1), 119–142.
- Leyffer, S., López-Calva, G., and Nocedal, J. (2006) *SIAM Journal on Optimization*, 17(1), 52–77.
- Leyffer, S. and Munson, T.S. (2007) *Preprint ANL/MCS-P1457-0907, Argonne National Laboratory, Mathematics and Computer Science Division*.
- Lin, G.H. and Fukushima, M. (2006) *Journal of optimization theory and applications*, 128(1), 1–28.
- Moudgalya, K.M. and Jaguste, S. (2001) *Chemical Engineering Science*, 56(11), 3611–3621.
- Moudgalya, K.M. and Ryali, V. (2001) *Chemical Engineering Science*, 56(11), 3595–3609.
- Nurkanović, A. and Diehl, M. (2022) *IEEE Control Systems Letters*, 6, 3110–3115.
- Nurkanović, A., Sperl, M., Albrecht, S., and Diehl, M. (2022) *arXiv preprint arXiv:2205.05337*.
- Patel, A., Shield, S.L., Kazi, S., Johnson, A.M., and Biegler, L.T. (2019) *IEEE Robotics and Automation Letters*, 4(2), 2242–2249.
- Raghunathan, A.U., Diaz, M.S., and Biegler, L.T. (2004) *Computers & chemical engineering*, 28(10), 2037–2052.
- Raghunathan, A.U., Jha, D.K., and Romeres, D. (2022) In *2022 International Conference on Robotics and Automation (ICRA)*, 985–991. IEEE.
- Ralph, D. and Wright, S.J. (2004) *Optimization Methods and Software*, 19(5), 527–556.
- Scheel, H. and Scholtes, S. (2000) *Mathematics of Operations Research*, 25(1), 1–22.
- Stewart, D. (1990) *Numerische Mathematik*, 58, 299–328.
- Wächter, A. and Biegler, L.T. (2006) *Mathematical programming*, 106, 25–57.